# PET 6-[18F]fluoro-L-m-tyrosine studies of dopaminergic function in human and nonhuman primates

**Jamie L. Eberling[1,2,*], Krystof S. Bankiewicz[3], James P. O'Neil[4] and William J. Jagust[1,5]**

1. Department of Molecular Imaging and Neuroscience, Lawrence Berkeley National Laboratory, Berkeley, CA, USA
2. Department of Neurology, University of California, Davis, CA, USA
3. Department of Neurological Surgery, University of California, San Francisco, CA, USA
4. Department of Molecular Imaging and Neuroscience, Lawrence Berkeley National Laboratory, Berkeley, CA, USA
5. Helen Wills Neuroscience Institute, University of California, Berkeley, CA, USA

Although positron emission tomography (PET) and the aromatic L-amino acid decarboxylase (AADC) tracer 6-[18F]fluoro-L-m-tyrosine (FMT) has been used to assess the integrity of the presynaptic dopamine system in the brain, relatively little has been published in terms of brain FMT uptake values especially for normal human subjects. Twelve normal volunteer subjects were scanned using PET and FMT to determine the range of normal striatal uptake values using Patlak graphical analysis. For comparison, seven adult rhesus monkeys were studied and the data analyzed in the same way. A subset of monkeys that were treated with a unilateral intracarotid artery infusion of the dopamine neurotoxin MPTP showed an 87% decrease in striatal FMT uptake. These findings support the use of PET and FMT to image AADC distribution in both normal and diseased brains using Patlak graphical analysis and tissue input functions.

Keywords: dopamine, FMT, Patlak, PET

## INTRODUCTION

Positron emission tomography (PET) has been used extensively to study the activity of aromatic L-amino acid decarboxylase (AADC) in the brains of both human and nonhuman primates. The most widely used tracer for the assessment of AADC continues to be 6-[18F]fluoro-L-DOPA (FDOPA). While FDOPA is well validated as a dopaminergic tracer (Eidelberg et al., 1994; Pate et al., 1993; Vingerhoets et al., 1994), it has the disadvantage of being subject to peripheral metabolism by catechol-O-methyltransferase (COMT). The resulting methylated metabolites are transported across the blood-brain barrier by the large neutral amino acid transporter and contribute to the PET signal in the brain thereby degrading the signal to noise ratio and complicating kinetic modeling (Doudet et al., 1991; Wahl et al., 1994). An alternative AADC tracer, 6-[18F]fluoro-L-m-tyrosine (FMT), is not subject to O-methylation resulting in better quality images with higher signal to noise and more straightforward kinetics (DeJesus et al., 1997; Jordan et al., 1997; Nahmias et al., 1995). We have used FMT extensively in the study of both normal and parkinsonian monkeys treated with the dopamine neurotoxin MPTP (Bankiewicz et al., 2006a,b; Eberling et al., 1997,

1998a, 2000, 2003; Forsayeth et al., 2006; Jordan et al., 1997) and have recently begun PET-FMT studies in normal human subjects and patients with Parkinson's disease (PD). Although FMT has been used previously by other groups, little has been published about its use in normal human subjects. The current report provides normative values for humans and monkeys. We also compared FMT uptake in monkeys before and after MPTP treatment as an animal model of PD in order to evaluate the use of this approach in an established disease model.

## MATERIALS AND METHODS

### Human studies

Twelve volunteers, 9 males and 3 females, between the ages of 41 and 58 were recruited by advertisement. All of the subjects were in good health, had no history of alcohol or drug abuse, and had not been treated for depression or any other neurological or psychiatric condition. Informed consent was obtained from the subjects after the nature of the experimental procedures was explained. All procedures were in accordance with the ethical standards of the institutional committee on human experimentation.

PET studies were performed on a Siemens ECAT EXACT HR PET scanner in 2D acquisition mode. FMT was synthesized using a semi-remote chemical synthesis apparatus (O'Neil and VanBrocklin, 1995) by a modification of a previously described procedure (Namavari et al., 1993). All subjects were studied approximately 60–90 minutes following an oral dose of 2.5 mg/kg of carbidopa. Subjects were positioned on the scanner bed and a thermoplastic mask was used to gently restrain the head. Prior to the emission scan a 10 minute transmission scan was obtained for attenuation correction. Subsequently, approximately 3–5 mCi of FMT was be injected as a bolus in an antecubital vein and a dynamic acquisition sequence was obtained: $12 \times 5$, $6 \times 10$, $4 \times 30$, $6 \times 60$,

$10 \times 300$ seconds. All procedures were performed in accordance with the National Institutes of Health guidelines and approved by the Human Subjects Quality Assurance Committee at the Lawrence Berkeley National Laboratory and the Committee for Protection of Human Subjects at the University of California at Berkeley.

## Monkey studies

Seven adult rhesus macaques (mean age $5.14 \pm 3.00$) were studied on the same PET scanner. Animals were anesthetized with an i.m. injection of ketamine (15 mg/kg), intubated and placed on methoxyflurane anesthesia. All animals were pretreated with an i.m. injection of benzerazide (2 mg kg), a peripheral decarboxylase inhibitor, 30 minutes before imaging. The animals were placed in a stereotaxic frame and positioned in the PET scanner. Images were obtained in the coronal plane. Transmission and emission data were collected in the same manner as the human studies but the emission scan lasted for 90 minutes. Since the human emission data were acquired for 60 minutes, only the first 60 minutes of the monkey emission data were used in the data analysis. A 10–15 mCi dose of FMT was injected simultaneously with the beginning of the emission scan. Five of the monkeys were studied in the same manner approximately 4 weeks after the unilateral intracarotid artery (ICA) infusion of MPTP as previously described in detail (Bankiewicz et al., 1986; Jordan et al., 1997). This results in a near complete unilateral lesion of the nigrostriatal pathway on the side of infusion and a hemiparkinsonian syndrome on the side contralateral to infusion. All procedures were in accordance with the National Institutes of Health guidelines and approved by the Animal Welfare and Research Committee at the Lawrence Berkeley National Laboratory.

## Data analysis

Data were reconstructed using an ordered subset expectation maximization (OSEM) algorithm with weighted attenuation, an image size of $256 \times 256$, and 6 iterations with 16 subsets. A Gaussian filter with 6-mm FWHM was applied, with a scatter correction.

PET data were quantified using a multiple time graphical analysis ("Patlak plot"). FMT data are amenable to this approach because FMT is an irreversibly bound tracer reaching steady state relatively quickly. These features, identical to those of FDOPA, define suitability for graphical analysis for an irreversible tracer as described by Patlak (Patlak and Blasberg, 1985) and previous studies have demonstrated the appropriateness of the Patlak model for the analysis of FMT data (Doudet et al., 1999; Jordan et al., 1997). FMT uptake can be quantified by $K_i$, which is the slope of linear fitting between two time-activity curves: the time-activity curve of a region of interest (ROI), in this case the striatum, and the time-activity curve of the blood input function (Patlak and Blasberg, 1985). The blood activity curve can be replaced by the time-activity curve of a reference region in which the tracer is nonspecifically bound, in this case the cerebellum (averaged over right and left hemispheres) (Dhawan et al., 2002; Lammertsma and Hume, 1996). Examples of time-activity curves for the striatum and cerebellum are shown in Figure 1. This approach has the obvious advantage of not requiring arterial blood sampling. Rather than $K_i$, FMT uptake in an ROI will be referred to as $K_i^c$ to denote that the cerebellum was used as the reference region. $K_i^c$ values were computed for the right and left striatum using ROIs drawn directly on the PET images. The Patlak model was fit with dynamic data from each ROI between 24 and 60 minutes, when the regression is highly linear ($r > 0.99$). Averaged $K_i^c$ values were calculated across all slices for each ROI. Thus, the conclusion of PET data reduction results in regional $K_i$ values for each subject, as well as a $K_i$ image in subject native space (see Figures 2 and 3).

Paired $t$-tests were used to compare $K_i^c$ values in the monkeys before and after MPTP treatment.

The uptake and washout of FMT is shown for the cerebellum and the right and left striatum for one of the human subjects. Both uptake and washout are rapid for the cerebellum, indicating nonspecific binding. The striatum shows continuous uptake, plateauing at about 20 to 30 minutes and without evidence of washout indicating specific binding in regions rich in dopaminergic neurons.
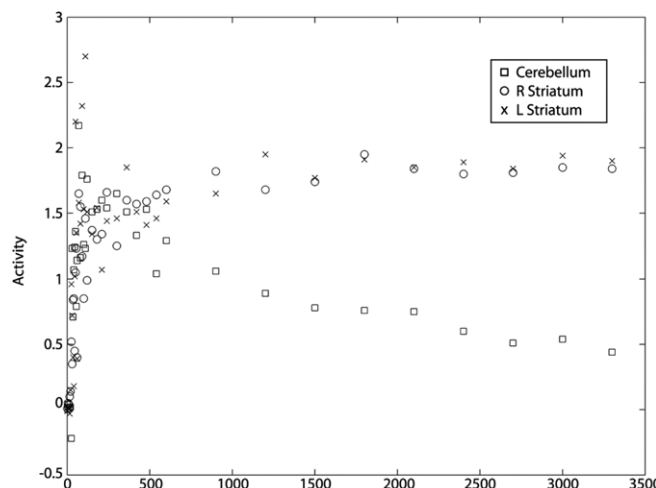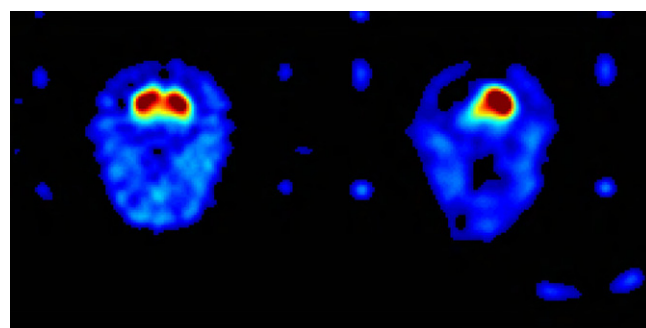


Figure 1. Time-activity curves.
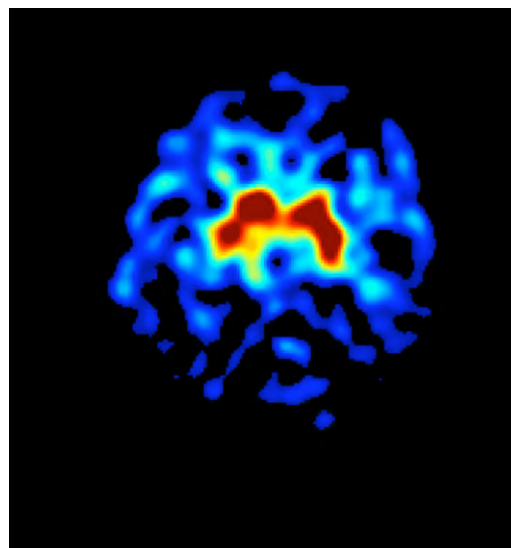


Figure 2. Human PET-FMT image.



Figure 3. Monkey PET-FMT images.

**Table 1. FMT uptake values in normal humans and monkeys.**

| Species | N | Input function | Striatal uptake Mean ± SD | COV (%) | Comments | Reference |
|---|---|---|---|---|---|---|
| Human | 12 | Cerebellar ROI | 0.021, 0.003 | 12 | Normal subjects Age 40–58 | |
| Human | 5 | Occipital ROI | 0.017, 0.002 | 12 | Normal subjects Age 18–25 years | Nahmias et al., 1995 |
| Human | 6 | Cerebellar ROI | 0.018, NA | NA | Normal subjects Mean age 26 ± 7 | Mamo et al., 2204 |
| Human | 4 | Cerebellar ROI | 0.019, 0.002 | 11 | Age 25–54 years | Asselia et al., 2002 |
| Human | 4 | Venous sinus ROI | 0.019, 0.005 | 26 | Age 25–54 years | Asselin et al., 2002 |
| Monkey | 7 | Cerebellar ROI | 0.022, 0.003 | 13 | Mean age 5.14 ± 3 | |
| Monkey | 6 | Arterial blood (metabolic corrected) | 0.013, 0.003 | 23 | Ages not available | Doudet et al., 1999 |
| Monkey | 6 | Occipital ROI | 0.013, 0.002 | 15 | Ages not available | Doudet et al., 1999 |
| Monkey | 3 | Occipital ROI | 0.017, 0.0006 putamen only | 3.5 | Ages 8, 9 and 30 years | Brown et al., 1999 |
| Monkey | 5 | Occipital ROI | 0.012, 0.003 | 25 | Age 3–13 years Partial volume correction | DeJesus et al., 2001 |
| Monkey | 5 | Occipital ROI | 0.014, 0.002 | 14 | Age 25–37 years Partial volume correction | DeJesus et al., 2001 |
| Monkey | 4 | Arterial blood (metabolic corrected) | 0.023, 0.006 | 26 | Age 5–10 years | Eberling et al., 2002 |
| Monkey | 6 | Arterial blood (metabolic corrected) | 0.018, 0.001 | 6 | Age 22–27 years | Eberling et al., 2002 |
| Monkey | 2 | Cerebellar ROI | 0.010, 0.00004 | 0.38 | MicroPET Age 7 years | DeJessus et al., 2005 |

**Table 2. FMT uptake values for individual human subjects.**

| Subject | Age | Gender | Striatal uptake |
|---|---|---|---|
| 1 | 53 | M | 0.019 |
| 2 | 41 | M | 0.022 |
| 3 | 46 | M | 0.019 |
| 4 | 55 | M | 0.025 |
| 5 | 41 | M | 0.021 |
| 6 | 52 | M | 0.017 |
| 7 | 50 | M | 0.023 |
| 8 | 58 | M | 0.019 |
| 9 | 40 | F | 0.017 |
| 10 | 46 | M | 0.023 |
| 11 | 50 | F | 0.024 |
| 12 | 49 | F | 0.021 |

## RESULTS

**Figure 2** shows a parametric image of striatal FMT uptake ($K_i$) for a 46-year-old human male.

The graphical method was implemented on a voxel-wise basis to produce calculated $K_i$ images using a cerebellar reference input. This axial image at the level of the striatum demonstrates high levels of tracer uptake in the striatum as shown in a 46-year-old male subject.

**Table 1** shows striatal FMT uptake ($K_i^c$) in normal humans and monkeys from this study as well as other published studies for comparison. **Table 2** shows individual $K_i^c$ values for the human subjects from this study in order to provide a comprehensive indication of the variability between subjects.

The striatal $K_i^c$ values reported from our laboratory tended to be higher than those reported from other laboratories for both humans and monkeys. FMT uptake values were more variable when calculated using blood input functions as shown by the coefficients of variation. $K_i^c$ values decreased significantly following unilateral MPTP treatment in monkeys ($t = 13.46$, $p < 0.001$), with reductions of 87% in the treated (left) hemisphere. **Figure 3** shows parametic images for a monkey studied before and after unilateral MPTP treatment.

Calculated $K_i$ images for a normal monkey (left) and the same monkey after unilateral left intracarotid artery infusion of the neurotoxin MPTP. Both images are coronal slices taken at the level of the striatum. Left striatal FMT uptake was reduced more than 80% following MPTP treatment.

## DISCUSSION

Our laboratory has extensive experience in FMT-PET imaging in normal and parkinsonian monkeys using several methods to analyze the data, including a 3-compartment tracer kinetic model, Patlak graphical analysis of tissue uptake, and a simple ratio approach (Eberling et al., 2004; Jordan et al., 1997). Our kinetic studies showed that brain radioactivity was in the form of 6-[$^{18}$F]fluoro-m-tryramine (FMA) and 6-[$^{18}$F]fluoro-3-hydroxyphenylacetic acid (FPAC), indicating a metabolic pathway consistent with decarboxylation of FMT to FMA and further metabolism by monoamine oxidase to FPAC. Results of primate studies using tracer kinetic modeling, Patlak graphical analysis, and simple striatum to cerebellum ratios were consistent with one another and showed substantial decarboxylation in regions of high dopamine content (caudate, putamen) (Eberling et al., 2004; Jordan et al., 1997). Here we report striatal FMT uptake in normal humans and monkeys using a multiple time graphical (Patlak) analysis. In addition, we report similar reductions in striatal FMT uptake in MPTP-treated monkeys as previously reported using various analytic methods supporting the use of this approach in both normal and diseased brains.

As shown in **Table 1** striatal uptake values tend to be more variable when using arterial blood vs. tissue input functions. Doudet et al. (1999)

reported more variability with arterial input functions than with tissue input functions (see **Table 1**). In fact, in general the studies that used image-derived tissue input functions, either the cerebellum or occipital cortex, showed less between subject variability than studies that used arterial input functions. Differences in uptake values between studies can likely be explained by differences in PET scanners and in the details of the analytic methods.

We considered measuring FMT values in cortical regions as well but opted not to because we were not confident that these measures are accurate. A number of studies (for review see Cropley et al. (2006)) have quantified FDOPA uptake in cortical areas, often in association with cognitive performance. However, the signal to noise ratio in the cortex is low for both FDOPA and FMT and the accuracy of cortical uptake values is uncertain (Cropley et al., 2006). We therefore chose to limit our analyses to the striatum.

The reductions in striatal FMT uptake we observed following unilateral intracarotid artery infusions of MPTP are similar to what we have previously observed using arterial input functions and kinetic modeling (Eberling et al., 1998b; Jordan et al., 1997). Here, we report an 87% reduction in striatal FMT uptake using a Patlak analysis. Doudet et al. (1999) previously reported that both FMT and FDOPA showed similar reductions in striatal uptake following MPTP treatment in monkeys. In addition, they reported negligible differences when comparing striatal FMT uptake values derived from arterial blood vs. occipital cortex input functions. Together, these findings support the use of the graphical analytic approach using a tissue input function for FMT studies of normal and impaired dopamine function. This approach has the obvious advantage of avoiding arterial blood sampling which is technically more demanding, more invasive, and less practical, especially in clinical settings.

While FDOPA is still the most commonly used tracer for the assessment of AADC, the quantification of FDOPA kinetics is significantly affected by the influence of peripheral metabolites that cross the blood-brain barrier. FMT is not subject to peripheral methylation by COMT resulting in higher quality brain images. In the brain, while FDOPA is decarboxylated by AADC into 6-[$^{18}$F]fluorodopamine (FDA), stored in vesicles, and subsequently metabolized by MAO and COMT, FMT is decarboxylated by AADC into FMA which has a low affinity for the vesicular transporter (Endres et al., 1997) and is thereby simply further metabolized by MAO into FPAC and trapped in the tissue. Thus, as previously suggested by Doudet et al. (1999), FMT is a superior tracer for the assessment of AADC, while FDOPA is the tracer of choice for assessing dopamine metabolism and turnover. FMT may be the tracer of choice for routine clinical studies because the images have higher target to background ratios and therefore higher contrast.

In summary, we report striatal FMT uptake values in normal humans and monkeys using cerebellar input functions and Patlak graphical analysis. Similar reductions in striatal FMT uptake were observed in MPTP treated monkeys using a Patlak graphical analysis to those reported previously using a arterial blood input functions and a kinetic modeling analytic approach (Eberling et al., 1998b; Jordan et al., 1997). These findings support the use of FMT to image AADC distribution using Patlak graphical analysis and tissue input functions for assessing the integrity of presynaptic dopamine function in normal and diseased brains. Although absolute uptake rates may range considerably depending upon the scanner, imaging protocol, and details of the analytic methods, relative rates appear to be similar when comparing studies done at different imaging centers.

## CONFLICT OF INTEREST STATEMENT

The authors declare that the research was conducted in the absence of any commercial or financial relationships that could be construed as a potential conflict of interest.

## REFERENCES

Bankiewicz, K. S., Daadi, M., Pivirotto, P., Bringas, J., Sanftner, L., Cunningham, J., Forsayeth, J. R., and Eberling, J. L. (2006a). Focal striatal dopamine may potentiate dyskinesias in parkinsonian monkeys. *Exp. Neurol.* 197, 363–372.

Bankiewicz, K. S., Forsayeth, J., Eberling, J. L., Sanchez-Pernaute, R., Pivirotto, P., Bringas, J., Herscovitch, P., Carson, R. E., Eckelman, W., Reutter, B., and Cunningham, J. (2006b). Long-term clinical improvement in MPTP-lesioned primates after gene therapy with AAV-hAADC. *Mol. Ther.* 14, 564–570.

Bankiewicz, K. S., Oldield, E. H., Chiueh, C. C., Doppman, D. M., Jacobowitz, D. M., and Kopin, I. J. (1986). Hemiparkinsonism in monkeys after unilateral internal carotid artery infusion of 1-methyl-4-phenyl-1,2,3,6-tetrahydropyridine (MPTP). *Life Sci.* 39, 7–16.

Cropley, V. L., Fujita, M., Innis, R. B., and Nathan, P. J. (2006). Molecular imaging of the dopaminergic system and its association with human cognitive function. *Biol. Psychiatry* 59, 898–907.

DeJesus, O. T., Endres, C. J., Shelton, S. E., Nickles, R. J., and Holden, J. E. (1997). Evaluation of fluorinated m-tyrosine analogs as PET imaging agents of dopamine nerve terminals: comparison with 6-fluoroDOPA. *J. Nucl. Med.* 38, 630–636.

Dhawan, V., Ma, Y., Pillai, V., Spetsieris, P., Chaly, T., Belakhlef, A., Margouleff, C., and Eidelberg, D. (2002). Comparative analysis of striatal FDOPA uptake in Parkinson's disease: ratio method versus graphical approach. *J. Nucl. Med.* 43, 1324–1330.

Doudet, D. J., Chan, G. L., Jivan, S., DeJesus, O. T., McGeer, E. G., English, C., Ruth, T. J., and Holden, J. E. (1999). Evaluation of dopaminergic presynaptic integrity: 6-[$^{18}$F]fluoro-L-dopa versus 6-[$^{18}$F]fluoro-L-m-tyrosine. *J. Cereb. Blood Flow Metab.* 19, 278–287.

Doudet, D. J., McLellan, C. A., Carson, R., Adams, H. R., Miyake, H., Aigner, T. G., Finn, R. T., and Cohen, R. M. (1991). Distribution and kinetics of 3-O-Methyl-6-[$^{18}$F]fluoro-l-DOPA in the rhesus monkey brain. *J. Cereb. Blood Flow Metab.* 11, 726–734.

Eberling, J. L., Bankiewicz, K. S., Jordan, S., VanBrocklin, H. F., and Jagust, W. J. (1997). PET studies of functional compensation in a primate model of Parkinson's disease. *Neuroreport* 8, 2727–2733.

Eberling, J. L., Cunningham, J., Pivirotto, P., Bringas, J., Daadi, M. M., and Bankiewicz, K. S. (2003). In vivo PET imaging of gene expression in Parkinsonian monkeys. *Mol. Ther.* 8, 873–875.

Eberling, J. L., Jagust, W. J., Taylor, S., Bringas, J., Pivirotto, P., VanBrocklin, H. F., and Bankiewicz, K. S. (1998a). A novel MPTP primate model of Parkinson's disease: neurochemical and clinical changes. *Brain Res.* 805, 259–262.

Eberling, J. L., Jagust, W. J., Taylor, S., Bringas, J., Pivirotto, P., VanBrocklin, H. F., and Bankiewicz, K. S. (1998b). A novel MPTP primate model of Parkinson's disease: neurochemical and clinical changes. *Brain Res.* 805, 259–262.

Eberling, J. L., Pivirotto, P., Bringas, J., and Bankiewicz, K. S. (2000). Tremor is associated with PET measures of nigrostriatal dopamine function in MPTP-lesioned monkeys. *Exp. Neurol.* 165, 342–346.

Eberling, J. L., Pivirotto, P., Bringas, J., and Bankiewicz, K. S. (2004). Comparison of two methods for the analysis of [$^{18}$F]6-fluoro-L-m-tyrosine PET data. *Neuroimage* 23, 358–363.

Eidelberg, D., Moeller, J. R., Dhawan, V., Spetsieris, P., Takikawa, S., Ishikawa, T., Chaly, T., Robeson, W., Margouleff, D., Przedborski, S., and Fahn, S. (1994). The metabolic topography of Parkinsonism. *J. Cereb. Blood Flow Metab.* 14, 783–801.

Endres, C. J., Swaminathan, S., DeJesus, O. T., Sievert, M., Ruoho, A. E., Murali, D., Rommelfanger, S. G., and Holden, J. E. (1997). Affinities of dopamine analogs for monoamine granular and plasma membrane transporters: implications for PET dopamine studies. *Life Sci.* 60, 2399–2406.

Forsayeth, J. R., Eberling, J. L., Sanftner, L. M., Zhen, Z., Pivirotto, P., Bringas, J., Cunningham, J., and Bankiewicz, K. S. (2006). A dose-ranging study of AAV-hAADC therapy in Parkinsonian monkeys. *Mol. Ther.* 14, 571–577.

Jordan, S., Eberling, J. L., Bankiewicz, K. S., Rosenberg, D., Coxson, P. G., VanBrocklin, H. F., O'Neil, J. P., Emborg, M. E., and Jagust, W. J. (1997). 6-[$^{18}$F]fluoro-L-*m*-tyrosine: Metabolism, PET kinetics, and MPTP lesions in primates. *Brain Res.* 750, 264–276.

Lammertsma, A. A., and Hume, S. P. (1996). Simplified reference tissue model for PET receptor studies. *Neuroimage* 4, 153–158.

Nahmias, C., Wahl, L., Chirakal, R., Firnau, G., and Garnett, E. S. (1995). A probe for intracerebral amino-acid decarboxylase activity: distribution and kinetics of [$^{18}$F]6-fluoro-L-m-tyrosine in the human brain. *Mov. Disord.* 10, 298–304.

Namavari, M., Satyamurthy, N., Phelps, M. E., and Barrio, J. R. (1993). Synthesis of 6-[$^{18}$F] and 4-[$^{18}$F]Fluoro-l-meta-tyrosines via regioselective radiofluorodestannylation. *Appl. Radiat. Isot.* 44, 527–536.

O'Neil, J. P., and VanBrocklin, H. F. (1995). Development of a semi-remote system for the routine production of [$^{18}$F]6-fluoro-L-meta-tyrosine to study striatal lesions and therapeutic implants in primates. *J. Labelled Comp. Radiopharm.* 37, 655–657.

Pate, B. D., Kawamata, T., Yamada, T., McGeer, E. G., Hewitt, K. A., Snow, B. J., Ruth, T. J., and Calne, D. B. (1993). Correlation of striatal fluorodopa uptake in the MPTP monkey with dopaminergic indices. *Ann. Neurol.* 34, 331–338.

Patlak, C. S., and Blasberg, R. G. (1985). Graphical evaluation of blood-to-brain transfer constants from multiple-time uptake data: generalizations. *J. Cereb. Blood Flow Metab.* 5, 584–590.

Vingerhoets, F. J., Snow, B. J., Lee, C. S., Schulzer, M., Mak, E., and Calne, D. B. (1994). Longitudinal fluorodopa positron emission tomographic studies of the evolution of idiopathic parkinsonism. *Ann. Neurol.* 36, 759–764.

Wahl, L., Chirakal, R., Firnau, G., Garnett, E. S., and Nahmias, C. (1994). The distribution and kinetics of [$^{18}$F]6-fluoro-3-O-methyl-L-dopa in the human brain. *J. Cereb. Blood Flow Metab.* 14, 664–670.